

A Pulse-density Modulation Circuit Exhibiting Noise Shaping with Single-electron Neurons

Andrew Kilinga Kikombo, Tetsuya Asai, Takahide Oya, Alexandre Schmid, Yusuf Leblebici and Yoshihito Amemiya

Abstract—We propose a bio-inspired circuit performing pulse-density modulation with single-electron devices. The proposed circuit consists of three single-electron neuronal units, receiving the same input and are connected to a common output. The output is inhibitorily feedback to the three neuronal circuits through a capacitive coupling, tuned to obtain a winners-share-all network operation. The circuit performance was evaluated through Monte-Carlo based computer simulations. We demonstrated that the proposed circuit possesses noise-shaping characteristics, where signal and noises are separated into low and high frequency bands respectively. This significantly improved the signal-to-noise ratio (SNR) by 4.34 dB in the coupled network, as compared to the uncoupled one. The noise-shaping properties are as a result of i) the inhibitory feedback between the output and the neuronal circuits, and ii) static noises (originating from device fabrication mismatches) and dynamic noises (as a result of thermally induced random tunneling events) introduced into the network.

I. INTRODUCTION

FOR the past 3 decades, the scaling of semiconductor devices has been the primary driving force behind improving the performance of LSI processors and systems. The decreasing feature sizes of transistors have been accompanied by dramatic increase in speed and integration densities, which have in turn led to increased and diversified functionality. This trend has been viable mainly due to guaranteed reliability in the downscaled devices even with decreasing process technologies. Reliability corresponds to high yields per die, hence low production costs (high cost efficiency), giving the circuit designer the opportunity to create reliable integrated systems with improved processing speeds, and increased functionality.

However, as the physical feature sizes approach the deep sub-micron regime, process variations and undesirable internal (and or external) noises associated with nano-scale properties pose critical concerns in the future of scaling and in system system design; they dramatically reduce the reliability of electronic devices on the edge of the nano-scales [1]. This reduced reliability is even more conspicuous as electronic device sizes are further scaled down to the nano-meter regime [2].

A.K. Kikombo, T. Asai, and Y. Amemiya are with the Graduate School of Information Science and Technology, Hokkaido University, Sapporo, 060-8628, Japan Email: kikombo@sapiens-ei.eng.hokudai.ac.jp

T. Oya is with the Graduate School of Engineering, Yokohama National University, Japan

A. Schmid, and Y. Leblebici are with the Microelectronic Systems Laboratory (LSM), Swiss Federal Institute of Technology (EPFL), Switzerland

Getting rid of these nano-scale characteristics would involve introducing error-detecting circuits within the system, which leads to advanced complexity, and design tradeoffs in using high integration capacities available to the circuit designer. Some design techniques offering possible ways to mitigate the impact of within-die variations have been explored [3]. Other works involving introduction of error-detecting circuitry in electronic systems include architectures proposed by Milor et. al [4] and Chatterjee [5]. Unfortunately, these approaches offer only a short term solution. The uncertainty in coming up with a long-lasting solution to these challenges has paved the way into a new field of the so called *emerging research nano devices*, which effectively utilize nano-scale characteristics in their operation. Such devices are viewed as promising blocks for creating application-specific processors, and ultra low-power systems in coming generations of LSI platforms. Such devices would include single-electron devices [6].

Single-electron devices inherently operate with extreme low power dissipation, and provide a high integration density per unit area. Thus, they are viewed as potential building blocks for low-power, parallel-based computational applications in future LSI platforms. However, one of the major problems facing single-electron devices is that they are potentially *unreliable*. Their low reliability originates from two factors: i) large variations in the features of fabricated devices, hence device characteristics, and ii) sensitivity to internal and external noises. Therefore, despite all the appealing features in utilizing nano-electronic devices in future electronic systems, we have to address and solve a fundamental question; how do we build reliable systems from error-prone building devices?

Improvements in fabrication technology alone cannot accommodate such enormous device failures. Therefore in designing functional electronic devices in the deep sub-micron and post-silicon era, we need to keep in mind the fact that we have to build *reliable* systems with *unreliable*, and error-prone devices [7] - [8]. Thus the need to address robustness and design systems with large enough signal-to-noise ratios is inevitable [9].

An innovative architectural approach to increasing reliability, is to exploit the internal and external noises, and the heterogeneity originating from fabrication mismatches in designing new electronic systems. For example, if we look at how living organisms code and transmit signals in their systems, we find similarities between neurons (the basic

elements responsible for information processing in neuronal systems) and nano-meter sized electronic devices. Neurons are sensitive to noises, operate asynchronously because of differences in their structural properties, and have large time jitters—that is, they are imperfect and unreliable [10]—but nevertheless they carry out information processing effectively. Similarly, nano-electronic devices (for instance single-electron devices) are sensitive to external interferences and noises, and have diverse fabrication variations in feature sizes, resulting in heterogeneity in parameters and device characteristics. Thus in creating electronic systems with such imperfect units, obtaining hints from living organisms is evidently of much importance. Such electronic systems that mimic neurological systems are referred to as *neuromorphic* circuits [11]. A number of neuromorphic circuits that operate by utilizing noises and device fabrication mismatches have been proposed. They include neuromorphic CMOS circuits utilizing device fabrication mismatches and environmental noises [12], single-electron circuits employing thermally induced stochastic resonance (SR) (see [13] for details on SR) in signal transmission [14], and single-electron networks performing synchrony detection [15].

This paper explores the possibility of creating novel circuit architectures with single-electron devices, by employing environmental (dynamic) noises, and static noises originating from fabrication mismatches. The circuit architecture is inspired by information coding mechanisms in biological neural networks that convert analog input signals into spike densities (digital-pulse streams) in the time domain. This operation is also referred to 1-bit analog-to-digital conversion, and is often implemented with $\Delta - \Sigma$ modulators. Such converters exhibit noise-shaping properties (see [16] for details on neuronal noise-shaping), separating signal and noises into low and high frequency bands respectively. A theoretical investigation of noise-shaping in neural networks is elaborated by Mar et. al [17]. In their work, they demonstrated that noise-shaping was improved by introducing an inhibitory coupling between noisy model integrate-and-fire neurons (IFNs). In addition, the authors note that the noise-shaping properties were improved due to heterogeneity and noises introduced into the network. Inspired by their work, we propose and investigate the performance of a single-electron pulse-density modulating circuit that exhibits noise shaping properties.

This paper is organised as follows. Firstly, a brief review of pulse-density modulation in neurons is presented. Secondly, implementation of integrate-and-fire neurons, together with fundamental operation of single-electron devices is illustrated. Thirdly, a model on how to realize pulse-density modulation employing excitatory and inhibitory mechanisms is explained. This is followed by the circuit structure implementing the model with single-electron oscillators. Fourthly, the performance of the proposed circuit is investigated through Monte-Carlo based computer simulations. The paper is summarized by noting on a possible architecture that also employs noises in achieving improved signal-to-noise ratio

in single-electron circuits and nanowire transistor networks.

II. A SHORT REVIEW OF PULSE-DENSITY MODULATION IN NEURONS

A neuron aggregates inputs from other neurons connected through synapses. The aggregated charge raises the membrane potential until it reaches a threshold, where the neuron fires generating a spike. This spike corresponds to a binary output “1”. After the firing event, the membrane potential is reset to a low value, and it increases again as the neuron accepts inputs from neighboring neurons (or input signals) to repeat the same cycle; producing a stream of “one” and “zero” pulse trains. The spike interval (density of spikes per unit time) is proportional to the analog input voltage i.e. the level of analog input is coded into pulse density. Thus a neuron can be considered as a 1-bit A-D converter operating in the temporal domain. Fig. 1(a) shows a schematic representation of analog-to-digital conversion in neurons. The output pulse density is proportional to the amplitude of the input signal. The operation of neurons is often modeled with spiking neurons such as the integrate-and-fire neurons. Fig. 1(b) illustrates the fundamental operation of an integrate-and-fire (IFN) neuron. The open circles (○) and shaded circles (●) represent excitatory and inhibitory synapses, respectively. The IFN receives input signals (voltages) through the excitatory synapses (to raise its membrane voltage) and inhibitory synapses (which decrease the membrane voltage) from adjacent neurons, to produce a spike if the summed input voltage ($\sum V_i^{\text{ex}} - \sum V_j^{\text{in}}$) exceeds the threshold voltage. After the IFN fires, its membrane voltage is reset to a low value, and the integration action resumes. The output pulse density is proportional to the net input voltage.

III. SINGLE-ELECTRON INTEGRATE AND FIRE NEURON

A single-electron oscillator [6], [18] is used to model the operation of an integrate-and-fire neuron (IFN). A single-electron oscillator (Fig. 2(a)) consists of a tunneling junction (capacitance = C_j) and a high resistance R connected in series at the node (●) and biased with a positive or a negative voltage V_d . It produces self-induced relaxation oscillations if the bias voltage is higher than the tunneling threshold ($V_d > e/(2C_j)$) (where e is the elementary charge and k_B is the Boltzmann constant). The node voltage V_1 increases as the capacitance C_j is charged through the series resistance (curve AB), until it reaches the tunneling threshold $e/(2C_j)$, at which an electron tunnels from the ground to the nanodot across the tunneling junction, resetting the node voltage to $-e/(2C_j)$. This abrupt change in node potential (from B to C) can be referred to as a firing event. The nanodot is recharged to repeat the same cycles. Therefore, a single-electron oscillator could be viewed as an integrate and fire neuron, which aggregates input voltages (or inputs from neighboring neurons) producing a pulse when its node voltage reaches the threshold voltage (Fig. 2(b)). By feeding a sinusoidal input to a single-electron oscillator, one can adjust the probability of electron tunneling in the circuit:

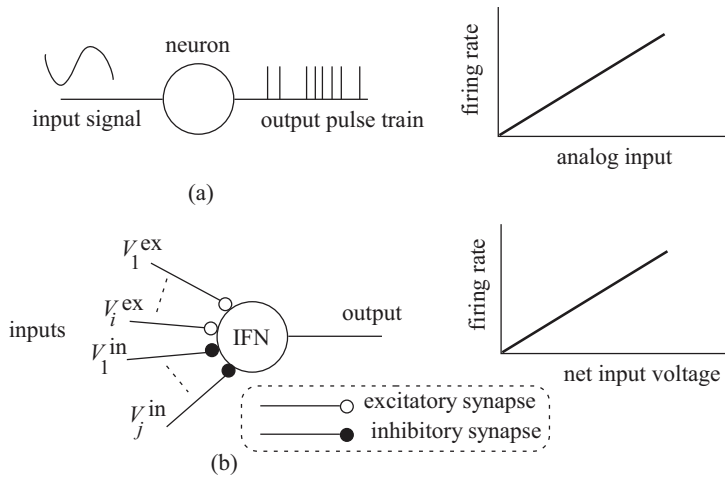


Fig. 1. (a) Pulse density modulation in neurons: analog input is converted into a pulse train whose density is proportional to the net amplitude of the input signal. (b) Fundamental structure and operation of integrate-and-fire neurons (IFNs). The IFN receives input voltages through excitatory and inhibitory synapses, and produces pulses when the net input voltage exceeds the threshold. The output pulse density (firing rate) is proportional to the net input voltage.

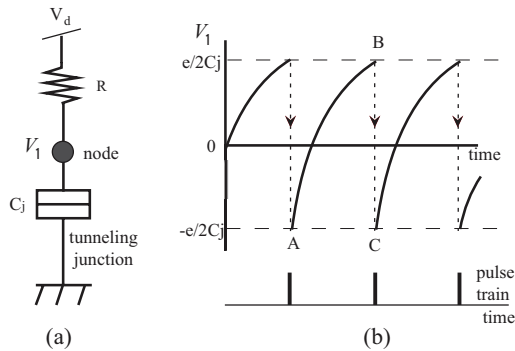


Fig. 2. Single-electron tunneling (SET) oscillator: (a) circuit configuration and (b) waveform showing oscillation of node voltage V_1 , as capacitor C_j is charged through resistance R (from A to B) and reset by an electron tunneling from the ground to the node (voltage drop from B to C). This sudden drop in the node voltage (BC) corresponds to a pulse output.

the tunneling rate increases as the input voltage rises above the threshold and gradually decreases to zero as the input approaches and falls below the threshold value. In other words, a single-electron oscillator converts an analog input into digital pulses. A single-electron oscillator can thus be viewed as a PDM converter, that produces a spike train (or produces zero) if the input signal exceeds (or falls below) the threshold value.

IV. CIRCUIT IMPLEMENTATION

Fig. 3 shows the model of the proposed circuit, consisting of three neuronal elements, the minimum number of units required to achieve a considerable signal-to-noise ratio ([12]). The neurons receive the same analog input through excitatory synapses (\circ) and produce digital pulses toward the global inhibitor Σ [19]. The output is fed-back to the three elements through inhibitory synapses denoted by shaded circles (\bullet) in the network. Firing in any of the neurons in the network

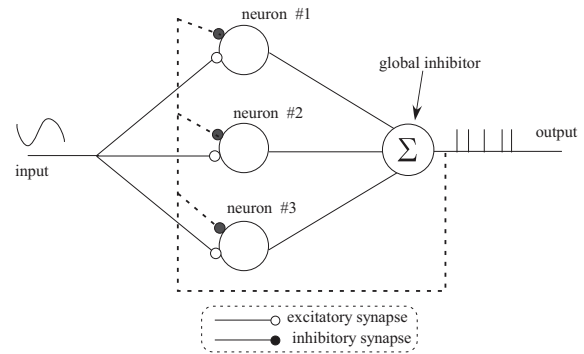


Fig. 3. Model of pulse-density modulation circuit employing excitatory and inhibitory mechanisms. A common input is fed to the three neurons through excitatory synapses (\circ), while the output is feedback to the three neurons through inhibitory synapses (\bullet).

decreases the membrane potential of the other neurons, reducing the probability of their firing.

The neuronal structure in Fig. 3 is implemented with single-electron oscillators that receive the same analog input. Each neuron in the network is implemented with a single electron oscillator. The input induces electron tunneling in the single-electron oscillators, generating pulses toward the global inhibitor. The global inhibitor (Σ) sums the pulses to produce a train of spikes representing tunneling (firing) events in the three neurons. Fig. 4 shows the circuit configuration. The global inhibitor is realized by numerically summing the firing events in the network. Inhibitory synapses are implemented by coupling capacitances (C), that decrease the node voltages of all the oscillators once a pulse is released at the output.

Each neuron in the network receives the same input ($V(t)$) raising its node voltage. Whenever any of the three single-electron oscillators reaches its threshold voltage, it fires, releasing a pulse toward the global inhibitor. The global in-

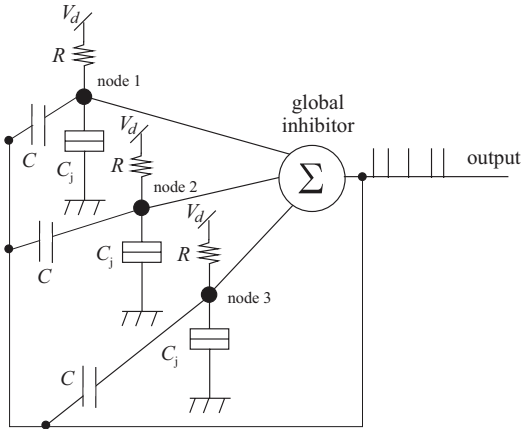


Fig. 4. Single-electron circuit performing pulse-density modulation. The structure consists of three single-electron oscillators, and a global inhibitor Σ . The output is fed back to all the other oscillators through the capacitive coupling C .

hibitor, through the coupling capacitors C , subtracts a certain amount of voltage from the other oscillators, suppressing them from tunneling for a certain period of time. This contributes to the distribution of output pulses. In the absence of the global inhibitor, all the neurons would fire randomly and with almost the same timing, producing a Poisson-like distribution of inter-spike intervals (ISIs). Contrarily, by introducing the global inhibitor, consecutive firing events in the network are suppressed, resulting in a Gaussian-like distribution of ISIs in the coupled network.

V. SIMULATION RESULTS

As mentioned in the introduction, the noise-shaping properties of the network of model neurons were reportedly improved by introducing dynamic and static noises [17]. In our circuit, this was realized as follows. As noted earlier, thermal noises lead to random electron tunneling in single-electron devices. We therefore introduced dynamical noises by tuning the temperatures in both the coupled and the uncoupled networks. Static noises were introduced only in the coupled network, by varying the values of series resistances R . In the coupled network, all the series resistances were set to 44 M Ω , whereas in the uncoupled network, the mean value of the three resistances was 44 M Ω (to obtain a ISI distribution with a standard deviation of one sigma), and the variance was $\pm 12.5\%$. The inhibitory coupling in the coupled network was implemented with a capacitive coupling of 4 aF. The temperature was set to 0.5 K in all simulations.

The performance of both the coupled and the uncoupled circuits was investigated through Monte-Carlo based computer simulations. All the circuit units in both the coupled and the uncoupled networks were fed with an input $V_d = 7.85$ mV.

Fig. 5 shows the raster plots of the firings of the network elements. The top diagrams of (a) and (b) show the random pulses for each unit in the uncoupled and coupled networks, respectively. The bottom diagrams in (a) and (b)

show the summed output (pulse train) for all the elements in the uncoupled and coupled networks, respectively. From the diagrams, we could observe that the firing timings in the uncoupled network were random and all the neurons fired with almost the same timing. In the coupled network, however, the firing of one of the neurons inhibited the others from firing, thus reducing the probability of consecutive firing in the network. In addition, the variance in the series resistances results in variations in the time constants of the network neurons. This reduced the probability of neurons attaining the firing threshold at the same time, and thus improved the distribution of firing intervals in the network. Consequently, these two factors resulted in well distributed firing timings in the network, leading to a Gaussian-like distribution of inter-spike intervals.

Fig. 6 shows the ISI distribution of firing events in the whole network. The histogram for the coupled network shows a Gaussian-like distribution with an inter-spike interval of 1.65 ns at the maximum number of firing counts. The histogram for the uncoupled network, in contrast, shows a Poisson-like distribution. We also investigated the effect of increasing the variance in the series resistances on the standard deviation of the Gaussian-like distribution. We found that the standard deviation increases as the variation decreases below or increases above 12.5%. As the variance decreases, the probability that multiple neurons in the network reach the threshold voltage at the same time increases. This shifts the ISI at the maximum firing rate toward zero, consequently leading to a larger standard deviation of the ISI distribution. The ISI distribution can, however, be tuned by adjusting the value of the inhibitory coupling capacitance C . As the coupling strength increases, the number of neurons reaching the threshold concurrently decreases drastically. In other words, the firing timings tend to distribute evenly, resulting to a sharper Gaussian-like distribution. However, increasing the coupling strength to a relatively high value, beyond the optimal value (of 4 aF in our simulations), leads to a winner-takes-all [20] operation (where only one neuron in the network produces the highest spike rate and inhibits all the others from firing). This would be undesirable, especially in a network of fault- and defect-prone elements, where increasing the probability of correct operation requires that all the elements play a substantial part in the network operation (i.e. a winners-share-all [21] operation, where several neurons in the network survive). Thus obtaining an ideal operation of the network requires tuning the firing rates of individual neurons through the series resistances, and also tuning the summed firing rate of the network through the capacitive coupling to obtain a winners-share-all type function.

Fig. 7 shows the power spectra for the coupled and uncoupled networks. The three neurons in both networks were fed with a sinusoidal input $V_d = V_0 + A\sin(2\pi ft)$, where amplitude $A = 2.5$ mV, frequency $f = 100$ MHz, and bias voltage $V_0 = 7.85$ mV. The power in both cases was calculated with 25 runs averaged with a square window. From

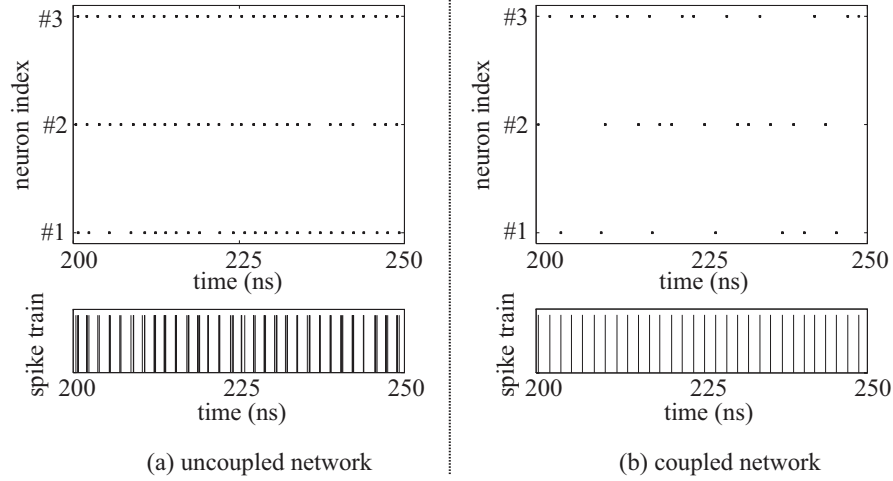


Fig. 5. Raster plots for firing events for uncoupled (left diagrams) and coupled (right diagrams) networks. The top diagrams show firing events for each neuron, while the bottom diagrams show summed output spike train at the global inhibitor Σ . Firing events in the uncoupled network were random and almost consecutive, whereas firing timings in the coupled network were well distributed as a result of the inhibitory coupling inhibiting concurrent events.

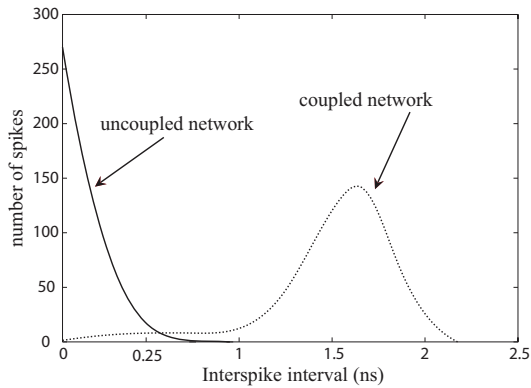


Fig. 6. Histogram of inter-spike intervals (ISIs) for coupled and uncoupled networks. The uncoupled network shows a Poisson-like distribution of ISIs where the firing events in the network elements are almost concurrent. The coupled network shows a Gaussian-like distribution, as a result of distributed firing events.

the results we can confirm that the global inhibitory coupling and the heterogeneity in series resistances collectively helped reduce the noise level in the coupled network substantially. The signal-to-noise ratio in the uncoupled network was 22.96 dB, while that in the coupled network was 27.30 dB below the cutoff frequency of 1 GHz. The harmonic distortions in the results are due to (i) the intrinsic firing rates of the individual neurons in the network and (ii) non-linear feedback introduced to the network. These distortions degraded the SNR characteristics. They could be decreased by setting the input signal frequency to a value much lower than the firing frequencies of individual neurons in the network. Another way of increasing the SNR without tuning the input frequency would be by filtering the output signals, to get rid of the higher frequencies. This is often realized with digital filters in the feedback loop of $\Sigma - \Delta$ converters

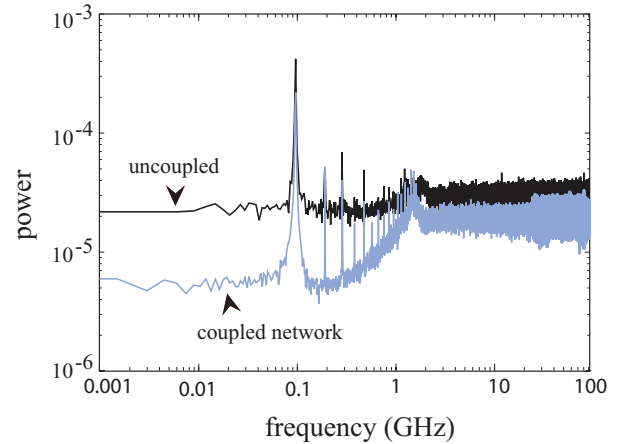


Fig. 7. Power spectra of coupled and uncoupled networks. The coupled network shows a reduced noise level in the lower frequencies (signal band), improving the SNR with 4.34 dB as compared to the uncoupled network.

[22].

VI. DISCUSSIONS AND CONCLUSION

To provide a basis for designing electronic circuits with mismatch-prone single-electron devices, this paper proposed and investigated the performance of a bio-inspired 1-bit analog-to-digital converter. The circuit elements are coupled to each other through a global inhibitory coupling. Through Monte-Carlo based computer simulations, we demonstrated that the presence of static and dynamic noises, and the global inhibitory coupling introduced into the circuit play an important role in improving its noise-shaping properties. The signal to noise ratio improved by 4.34 dB in the coupled network as compared to the un-coupled one.

In the present network we extensively investigated the

effect of static noises as a result of variations in series resistances, and of the inhibitory coupling in the network to noise-shaping properties. Investigating the effect of dynamic noises at higher temperatures, would also give a guideline into actual circuit design with such noise sensitive devices. From the results of these investigations, we can deduce that the performance of the circuit would improve up to an optimal value of thermal noises, and then deteriorate drastically as randomly induced firing further increases. This is as a result of decreased effect of the inhibition strength which contributes to the Gaussian-like distribution as discussed in the simulation results.

Also, choosing the optimal number of neurons to use in the network would play an important role in improving its performance. As the number of neurons increases, we would obtain better resiliency toward faults and defects in the network. This would however, come at the expense of tuning the optimal inhibitory coupling strength to realize a winners-share-all operation.

Before summarizing the paper, it's worth noting on similar promising works in achieving robust electronic systems by utilizing noises in improving signal-to-noise ratio in electronic systems. This approach has been demonstrated with single-electron devices, and nanowire transistor networks [23] by some of the authors of this paper. The architectures effectively employ stochastic resonance (SR) [13], and demonstrate a viable novel approach to realizing robust systems in noisy environments. Stochastic resonance is a phenomenon where weak signals can be retrieved from a noisy output [24] by applying an optimal amount of random noise. Oya et. al., [14] proposed a single-electron neural network that utilizes SR in signal transmission in neural networks, and successfully demonstrated that using SR indeed improved the temperature performance of the circuit. Kasai et. al. [23] experimentally investigated the performance of nanowire transistors with variations in threshold voltages and operating in a noisy experimental setup. In both cases, the effects of SR were investigated by setting the input signal to a value lower than the tunneling (firing) threshold of the network elements. By applying noises, network elements with non-zero inputs were induced to tunnel—tunneling events synchronized with the input signal to a certain quantity of noises. The authors showed that the SNR in their circuits was enhanced through partially using noises.

Such innovative approaches, in addition to the neuro-morphic methodology described in this paper would be indispensable in addressing reliability issues in electronic circuitry with nano-electronic devices. From the investigation results in this paper, we can conclude that by learning from biological systems: high levels of redundancy where information processing depends on many neurons operating in parallel, controlled signal transfer through excitatory and inhibitory synapses, and stochastic resonance mechanisms, we could get hints on how to design circuits that perform better even in noisy environments and (or) with failure-prone electronic devices.

REFERENCES

- [1] C., Constantinescu, "Trends and challenges in VLSI circuit reliability," *IEEE Micro*, vol. 23, pp. 14–19, 2003.
- [2] P.A. Stolk, F.P. Widdershoven, and D.B.M. Klaassen, "Modeling statistical dopant fluctuations in MOS transistors," *IEEE Trans. Electron Devices*, vol. 45, pp. 1960–1971, 1998.
- [3] D. Marculescu, and E. Talpes, "Variability and energy awareness: A microarchitecture-level perspective," *Proc. of the 42nd annual conf. on Design Automation (DAC)*, pp. 11–16, 2005.
- [4] L. Milor, and V. Visvanathan, "Detection of catastrophic faults in analog integrated circuits," *IEEE Transactions on Computer-Aided Design of Integrated Circuits and Systems*, vol. 8, pp. 114–130, 1989.
- [5] A. Chatterjee, "Concurrent Error Detection and Fault-Tolerance in Linear Analog Circuits Using Continuous Checksums," *IEEE Transactions on very large scale Integration (VLSI) Systems*, vol. 1, pp. 138–150, 1993.
- [6] H. Grabert, and M.H. Devoret, *Single Charge Tunneling—Coulomb Blockade Phenomena in Nanostructures*. Plenum, New York, 1993.
- [7] K. Nikolic, A. Sadek, and M. Forshaw, "Architectures for reliable computing with unreliable nanodevices," *Proceedings of the 2001 1st IEEE IEEE-NANO Nanotechnology conference*, pp. 254–259, 2001.
- [8] A. Schmid, and Y. Leblebici, "Robust circuit and system design methodologies for nanometer-scale devices and single-electron transistors," *IEEE Transactions on Very Large Scale Integration (VLSI) Systems*, vol. 12, pp. 1156–1166, 2004.
- [9] H. Hamed, Single electron devices: challenge for nanofabrication," *J. of vac. Sci & Tech.*, vol. 15, pp. 2101–2108, 1997.
- [10] M.N. Shadlen, and W.T. Newsome, "The Variable Discharge of Cortical Neurons: Implications for Connectivity, Computation, and Information Coding," *J. of Neuroscience*, vol. 18, pp. 3870–3896, 1998.
- [11] C. Mead, *Analog VLSI and neural systems*. Addison Wesley, New York, 1989.
- [12] A. Utagawa, T. Asai, T. Hirose, and Y. Amemiya, "An inhibitory neural-network circuit exhibiting noise shaping with subthreshold MOS neuron circuits," *IEICE Transactions on Fundamentals of Electronics, Communications and Computer*, E90-A, pp. 2108–2115, 2007.
- [13] J.J. Collins, C.C. Chow, T.T. Imhoff, "Stochastic resonance without tuning," *Nature*, vol. 376, pp. 236–238, 2002.
- [14] T. Oya, T. Asai, and Y. Amemiya, "Stochastic resonance in an ensemble of single-electron neuromorphic devices and its application to competitive neural networks," *Chaos, Solitons & Fractals*, vol. 32, pp. 855–861, 2007.
- [15] T. Oya, T. Asai, R. Kagaya, T. Hirose, and Y. Amemiya, "Neuronal synchrony detection on single-electron neural network," *Chaos, Solitons & Fractals*, vol. 27, pp. 887–894, 2006.
- [16] C. Mayr, and R. Schueffny, "Applying Spiking Neural Nets to Noise Shaping," *IEICE - Transactions on Information and Systems*, E88-D, pp. 1885–1892, 2005.
- [17] D.J. Mar, C.C. Chow, W. Gerstner, R.W. Adams, and J.J. Collins, "Noise shaping in populations of coupled model neurons," *Neurobiology*, vol. 96, pp. 10450–10455, 1999.
- [18] T. Oya, T. Asai, T. Fukui, and Y. Amemiya, "Reaction-diffusion systems consisting of single-electron circuits," *Inter. J. of Unconventional Computing*, vol. 1, pp. 177–194, 2005.
- [19] T. Asai, Y. Kanazawa, and Y. Amemiya, "A subthreshold MOS neuron circuit based on the volterra System," *IEEE transactions on neural networks*, vol. 14, no. 5, pp. 1308–1312, 2003.
- [20] M.A. Cohen, and S. Grossberg, "Absolute stability of global pattern formation and parallel memory storage by competitive neural networks," *IEEE Transactions on Systems, Man and Cybernetics*, vol. 13, pp. 815–826, 1983.
- [21] T. Fukai, and S. Tanaka, "A simple neural network exhibiting selective activation of neuronal ensembles: from winner-take-all to winners-share-all," *Neural Computation* vol. 9, pp. 77–97, 1997.
- [22] Y-G. Kim, and J-K, Kwon, "Multi-bit Sigma-Delta Modulator for Low Distortion and High-Speed Operation," *ETRI Journal*, vol. 29, pp. 835–837, 2007.
- [23] S. Kasai and T. Asai, "Stochastic resonance in Schottky wrap gate-controlled GaAs nanowire field effect transistors and their networks," *Applied Physics Express*, vol. 1, 083001, 2008.
- [24] L. Gammaitoni, P. Hanggi, P. Jung, and F. Marchesoni, "Stochastic resonance," *Reviews of Modern Physics*, vol. 70, pp.223-287, 1998.